Detection Schemes for ATSC 3.0 Transmitter Identification in Single Frequency Network

Sunhyoung Kwon, *Member, IEEE*, Sung-Ik Park, *Senior Member, IEEE*, Jae-Young Lee, *Senior Member, IEEE*, Bo-Mi Lim, *Member, IEEE*, Sungjun Ahn, *Member, IEEE*, and Joonhyuk Kang, *Member, IEEE*

***Abstract*—Single frequency network (SFN) enables efficient use of spectrum by allocating the same frequency among multiple transmitters. In order to efficiently design and manage the SFN, the Advanced Television Systems Committee (ATSC) 3.0 physical layer standard has adopted transmitter identification (TxID) technology which allows to measure the individual and/or whole network channel response, such as power and time delay of the broadcast signal from transmitters. Since TxID is embedded into the host ATSC 3.0 frame as radio frequency (RF) watermark, it is transparent to legacy ATSC 3.0 receivers and only a specially designed TxID analyzer is able to detect it. This paper presents new TxID detection methods that improve the detection performance of ATSC 3.0 TxID signal by resolving the problems and limitation of the conventional TxID detection method. The superiorities of the proposed detection methods are verified through computer simulation, laboratory test, and field trial.**

***Index Terms*—ATSC 3.0, transmitter identification, SFN.**

I. Introduction

THE NEXT generation terrestrial broadcasting standard, called the Advanced Television Systems Committee (ATSC) 3.0 [1], has been finalized in 2018. This new standard has been developed to meet the rapidly growing demands for broadcasters' intended services such as mobile/indoor reception, advanced emergency alerting services, ultra-high-definition (UHD) television (TV) services, and Internet protocol (IP) based interactive services.

The physical layer standard of ATSC 3.0 has been developed to provide enhanced robustness and extended flexibility as well as better spectrum efficiency [2]–[4]. The ATSC 3.0 physical layer signal consists of two parts: bootstrap and orthogonal frequency division multiplexing (OFDM) based data part. The bootstrap, known as universal entry point, is the first portion of the ATSC 3.0 RF frame structure and contains the necessary information to demodulate the remaining data part [5]. The bit interleaved coding and modulation (BICM) scheme has been adopted for OFDM based data part. This BICM offers not only enhanced robustness, but also extended flexibility enabling a wider range of operating modes compared to existing terrestrial standards [6], [7]. For multiple media services with different quality of service (QoS), three kinds of multiplexing schemes have been adopted: time division multiplexing (TDM), frequency division multiplexing (FDM), and layered division multiplexing (LDM). LDM is a novel multiplexing technique that combines different services with different power levels, and provide significant performance improvement compared to other multiplexing schemes [8]–[11].

Another approach to dramatically improving spectrum utilization is to use a single frequency network (SFN) where all transmitters in the same SFN are operated on the same frequency. To design and manage SFN efficiently, ATSC 3.0 physical layer standard has adopted transmitter identification (TxID) technology which allows to measure channel response, such as power and time delay, of all transmitters and/or individual transmitter in SFN. Note that the TxID is transparent to the legacy ATSC 3.0 receivers because it is embedded into the host ATSC 3.0 frame as radio frequency (RF) watermark. By detecting TxID, SFN information such as power and time delay of individual transmitters can be easily acquired without turning on and off each transmitter. However, in terms of TxID signal detection capability, the conventional auto- and cross-correlation based TxID detection algorithm, which is being used in ATSC 1.0 TxID detection, provides limited performance for ATSC 3.0 because frame structures and TxID insertion of ATSC 3.0 are not the same as ATSC 1.0. This paper presents a basic procedure of TxID insertion into the host ATSC 3.0 frame and analyzes theoretical TxID detection performance. Furthermore, in order to overcome problem and limitation of the existing TxID detection algorithm, three novel detection methods are proposed and verified through computer simulation, laboratory test, and field trial.

Manuscript received March 26, 2019; accepted April 12, 2019. Date of publication October 15, 2019; date of current version June 5, 2020. This work was supported by the Institute of Information and Communications Technology Planning and Evaluation grant funded by the Korea Government (MSIT, Development of ATSC 3.0-Based On-Channel Repeater Technology for High Quality Broadcasting) under Grant 2019-0-00030. *(Corresponding author: Joonhyuk Kang.)*

S. Kwon is with the Department of Electrical Engineering, Korea Advanced Institute of Science and Technology, Daejeon 34141, South Korea, and also with the Broadcasting Systems Research Department, Electronics and Telecommunications Research Institute, Daejeon 34129, South Korea (e-mail: shkwon@etri.re.kr).

S.-I. Park, J.-Y. Lee, B.-M. Lim, and S. Ahn are with the Broadcasting Systems Research Department, Electronics and Telecommunications Research Institute, Daejeon 34129, South Korea (e-mail: psi76@etri.re.kr; jaeyl@etri.re.kr; blim_vrossi46@etri.re.kr; sjahn@etri.re.kr).

J. Kang is with the Department of Electrical Engineering, Korea Advanced Institute of Science and Technology, Daejeon 34141, South Korea (e-mail: jhkang@ee.kaist.ac.kr).

Color versions of one or more of the figures in this article are available online at http://ieeexplore.ieee.org.

Digital Object Identifier 10.1109/TBC.2019.2941074

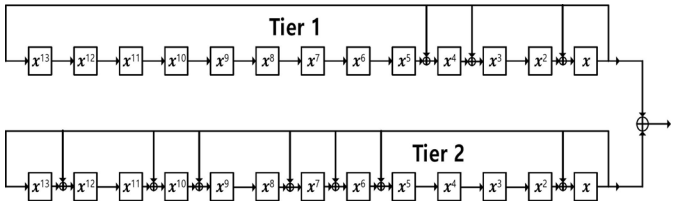

Fig. 1. Gold sequence generator for TxID signal.

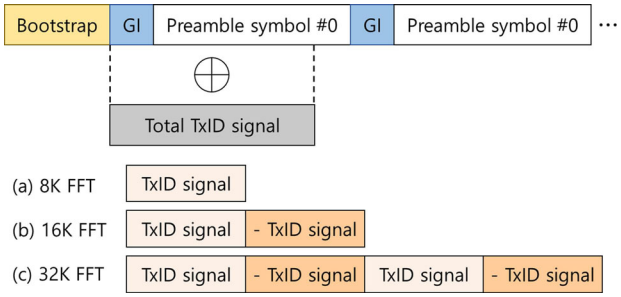

Fig. 2. TxID signal injection for various FFT sizes.

The remaining of this paper is organized as follows: In Section II, the generation and insertion procedure of ATSC 3.0 TxID are described. In Section III, the theoretical and mathematical performance analysis in terms of upper bound and detection performance are performed. Section IV describes the frame structure of ATSC 3.0 system and presents its negative impact on TxID detection performance. In Section V, three novel detection methods are proposed to improve the TxID detection performance taking into account implementation complexity. In Section VI, the superiorities of the three proposed methods are verified through extensive computer simulation, laboratory test, and field trial. The final conclusion of this paper is presented in Section VII.

II. Transmitter Identification

In SFN environments, when SFN signals from multiple transmitters are received, it is difficult to distinguish individual transmitters among the received signals. This is because each transmitter in the same SFN transmits perfectly the same signal so that the signals from multiple transmitters do not interfere with each other. In ATSC 3.0 system, for identification of individual transmitters, different RF watermarking patterns are inserted to each transmitter, which allows to manage and monitor the status of each transmitter in an SFN, without the hassle of turning on and off each transmitter.

The ATSC 3.0 TxID technology is a kind of direct sequence buried spread spectrum RF watermark technologies [12]–[14], similar to the ATSC 1.0 TxID insertion method. In ATSC 3.0 system, Gold code sequence [15] is used to generate the RF watermark signal. Each transmitter has a unique Gold code sequence so that the Gold code sequence will identify individual transmitters in SFN. The RF watermark signals are injected into the host ATSC 3.0 signal during the first preamble symbol period only. ATSC 3.0 provides several options for the injection level of the TxID signal, allowing the injection level to be chosen appropriately by broadcasters for each broadcasting environment.

A. Generation of TxID Signal

To generate TxID signal, Gold sequence, a special form of pseudo random noise (PN) sequences, is used in ATSC 3.0. The Gold sequences exist if and only if the length of the sequence is $2^n - 1$ for $n \neq 0 \ mod \ 4$ [15]. In ATSC 3.0, the Gold sequence has a length of 8191 ($n = 13$) so that the Gold sequence based TxID signal can be inserted into the first preamble symbol period regardless of preamble configuration.

The sequence is generated by a pair of primitive polynomials and shift registers that have the lengths, feedback paths, and summing functions defined in Figure 1. The two shift registers are defined by the following generator polynomials, respectively:

- Generator polynomial for Tier 1: $x^{13} + x^4 + x^3 + x + 1$
- Generator polynomial for Tier 2: $x^{13} + x^{12} + x^{10} + x^9 + x^7 + x^6 + x^5 + x + 1$

For generating the Gold sequence, each of the two shift registers in Figure 1 are preloaded for each frame so that TxID signal is the same for every frame. The shift registers in Tier 1 are preloaded with a value of 1 in the x stage and 0 in all the other stages. For the shift registers in Tier 2, a 13-bit TxID address value is preloaded into the x^{13} through x stages where the most significant bit is mapped into x^{13} stage and the least significant bit into the x stage. A TxID address value is uniquely assigned to each transmitter on a given RF channel so that this value can be used for controlling each individual transmitter by the scheduler. Thus, the number of possible TxID address values being assigned to individual transmitters is $2^{13} = 8192$.

The combined output of the two shift registers is modulated by binary phase shift keying (BPSK) modulator before injecting into the host ATSC 3.0 preamble symbol. If the combined output bit is 'zero', then it is modulated as '-1'. If the combined output bit is 'one', then it is modulated as '$+1$'. As a result, the generated TxID signal is the BPSK modulated signal with a length of 8191 samples.

B. TxID Signal Injection

The generated TxID signal is injected into the first preamble symbol period in time domain and transmitted simultaneously with the host ATSC 3.0 signal. To minimize the negative impact on data part in ATSC 3.0 frame such as audio and video contents due to TxID injection, the TxID signal is injected in preamble period only which is more robust than data part. The injection level of TxID should be carefully chosen by the broadcasters to minimize the performance impact of the host broadcasting signals while maintaining the detection performance of TxID signal in the receiving side such as a measurement or monitoring equipment.

The beginning of the TxID signal is always exactly aligned with the first sample of the first preamble symbol including the symbol's guard interval (GI), as depicted in Figure 2. However, since the symbol period is determined by the fast Fourier transform (FFT) size, the TxID signal can be inserted multiple times within one preamble symbol to maximize the

TxID detection capability. When an 8K FFT size is used for the preamble, the TxID having the length of 8191 samples is injected once per an ATSC 3.0 frame as depicted in Figure 2 (a). For the 16K FFT, the duplicated TxID signal is additionally injected within the first preamble symbol period as depicted in Figure 2 (b). The duplicated TxID signal has the opposite polarity to the first TxID signal in order to average out DC components of the total TxID signal. When the 32k FFT size is used for the preamble, the TxID signal is repeated four times as depicted in Figure 2 (c). In this case, the second and fourth TxID signals have the opposite polarities to the first and third TxID signals.

III. Theoretical Performance Analysis of TxID Signal

The ATSC 3.0 TxID technology is a kind of spread spectrum techniques, more specifically direct sequence spread spectrum (DSSS). Spread spectrum is typically designed to be transparent to other users, except for the designated users, and it is difficult to determine whether a spread spectrum signal is actually present. This technique has been widely used for several decades in military communications due to this property. Code Division Multiple Access [16] is another example of successful use for spread spectrum technique, where efficient use of spectrum was also considered. This DSSS approach has been adopted in ATSC 3.0 TxID because ATSC 3.0 ordinary TV receivers do not need to detect and decode TxID signals while only special broadcasting equipment is capable of detecting and decoding it. In Section III-A, the processing gain of the ATSC 3.0 TxID technique is analyzed in the viewpoint of DSSS system. In order to reliably detect TxID signal, an appropriate injection level should be selected according to the broadcasting environment. Otherwise, a transmitter closely located in the receiver may cause overwhelming interference which results in the detection failure of TxID signal from other transmitters. To account for this realistic broadcasting environment, the theoretical detection performance of TxID signal in a situation where a plurality of ATSC 3.0 signals have different reception power levels is mathematically analyzed in Section III-B.

A. Theoretical Upper Bound (Processing Gain)

In a DSSS system, a data symbol is spread over much higher bandwidth by multiplying with a PN sequence. The user data symbol rate (R_s) is always relatively low compared to the rate of the PN sequence, called chip rate (R_c). The processing gain can be obtained by spreading at transmitter and despreading again at receiver, and it is defined as the ratio of chip rate to the user data symbol rate:

$$\textit{processing gain}\ [\text{dB}] = 10\log_{10}(R_c/R_s)$$

For ATSC 3.0 system, the Gold code sequence has been chosen as a PN sequence because of its good auto- and cross-correlation properties with large family size, which offers sufficient capability to identify a huge number of transmitters. The Gold code sequence used in ATSC 3.0 has a length of 8191 so that one TxID symbol consists of 8191 chips where each chip is a rectangular pulse of $+1$ or -1 amplitude. Therefore, the processing gain of ATSC 3.0 TxID signal can be calculated as $10 * \log_{10}(8191/1) = 39.1334$ dB. This indicates the theoretical upper bound of detection performance of the Gold sequence used in ATSC 3.0.

B. Theoretical Detection Performance Analysis of TxID in SFN

Let ATSC 3.0 host signal and TxID signal from i-th transmitter at time k be $d(k)$ and $x_i(k)$, respectively. The host signal $d(k)$ is assumed to be independent and identically distributed (i.i.d.) random variable with zero-mean and unit variance (i.e., unit power in average). Then, TxID signal embedded ATSC 3.0 signal, $d_i(k)$, can be represented as

$$d_i(k) = d(k) + \alpha_i \cdot x_i(k) \tag{1}$$

where α_i is a scaling factor corresponding to an injection level of the i-th transmitter. Then, the received signals, $r(k)$, at the TxID analyzer can be represented as

$$r(k) = \sum_{i=1}^{T} [\beta_i \cdot d_i(k - k_i) \otimes h_i] + w(k)$$

where h_i is a channel normalized to unity between the TxID analyzer and the i-th transmitter, k_i and β_i are a relative arrival time and magnitude of the received signal from 1st and i-th transmitters, T is number of transmitters, $\otimes$ is a convolution operation, and $w(k)$ is an additive white Gaussian noise (AWGN) with zero-mean and a variance of σ^2, respectively. Assuming that the received signals are synchronized and normalized with the signal from the 1st transmitter, k_1 and β_1 are 0 and 1, respectively.

The cross-correlation $R_{r,x_j}(\tau)$ between the received signal and the j-th transmitter's TxID signal can be represented as

$$\begin{aligned}
R_{r,x_j}(\tau) &= \frac{1}{M}\sum_{k=0}^{M-1} r(k)\cdot x_j(\tau - \mathrm{k}) \\
&= \frac{1}{M}\left\{\sum_{k=0}^{M-1} \alpha_j\beta_j \cdot x_j\big(k - k_j\big)\cdot x_j(\tau - \mathrm{k})\right\} \otimes h_j \\
&\quad + \frac{1}{M}\left\{\sum_{i=1, i\neq j}^{T}\sum_{k=0}^{M-1} \alpha_i\beta_i \cdot x_i(k - k_i)\cdot x_j(\tau - \mathrm{k})\right\} \otimes h_i \\
&\quad + \frac{1}{M}\sum_{k=0}^{M-1}\left\{\sum_{i=1}^{T}[\beta_i \cdot d(k - k_i)\otimes h_i] + w(k)\right\}\cdot x_j(\tau - \mathrm{k}) \\
&= \alpha_j\beta_j \cdot R_{x_j,x_j}(\tau)\otimes h_j + \sum_{i=1, i\neq j}^{T} \alpha_i\beta_i \cdot R_{x_i,x_j}(\tau)\otimes h_i \\
&\quad + \frac{1}{M}\sum_{k=0}^{M-1}\left\{\sum_{i=1}^{T}[\beta_i \cdot d(k - k_i)\otimes h_i] + w(k)\right\}\cdot x_j(\tau - \mathrm{k})
\end{aligned} \tag{2}$$

where M is the length of the Gold sequence. Owing to the small cross-correlation property of Gold sequence, $R_{x_i,x_j}(\tau) \cong 0$ can be reasonably assumed for $i \neq j$. It hence

yields (2) to be

$$R_{r,x_j}(\tau) \cong \alpha_j\beta_j \cdot R_{x_j,x_j}(\tau) \otimes h_j + \frac{1}{M} \times \sum_{k=0}^{M-1} \left\{ \sum_{i=1}^{T} [\beta_i \cdot d(k-k_i) \otimes h_i] + w(k) \right\} \cdot x_j(\tau - k) \tag{3}$$

Let the desired TxID signal be received at $c \in \Lambda$ where $\Lambda = \{c_1,\ c_2,\ \ldots, c_L\}$ is a set of arrival times for the desired TxID signal through channel with L number of multi-paths. Then, $R_{r,x_j}(c)$ for c $\in \Lambda$ is correlation value of the desired TxID signal while $R_{r,x_j}(\mu)$ for $\mu \notin \Lambda$ is that of the interference plus noise. For a performance measurement metric, TxID signal-to-interference-plus-noise ratio (TINR) is defined as follows;

$$\text{TINR} = 10\log_{10} \frac{\sum_{\text{c}\in\Lambda} E\left\{ \left| R_{r,x_j}(c) \right|^2 \right\}}{\sum_{\mu\notin\Lambda} E\left\{ \left| R_{r,x_j}(\mu) \right|^2 \right\} / (W-L)} \tag{4}$$

where W is the time window size for searching TxID signal, L is the number of multipath. It should be noted that L correlation values corresponding to the desired signals are summed to obtain the received signal power in total. On this other side, W-L correlation values corresponding to the interference plus noise are averaged to obtain the average power level of the interference plus noise. For AWGN channel, by using the property of $E\{|h_j|^2\} = 1$, $E\{|R_{r,x_j}(\tau)|^2\}$ can be simplified as

$$E\left\{ \left| R_{r,x_j}(\tau) \right|^2 \right\} = \left(\alpha_j\beta_j \right)^2 \cdot E\left\{ \left| R_{x_j,x_j}(\tau) \right|^2 \right\} + \frac{1}{M^2} \times E\left\{ \left| \sum_{k=0}^{M-1} \left\{ \sum_{i=1}^{T} [\beta_i \cdot d(k-k_i) \otimes h_i] + w(k) \right\} \cdot x_j(\tau - \text{k}) \right|^2 \right\} \tag{5}$$

Then, the 2nd term of (5) can be expanded as follows;

$$\begin{aligned} &\frac{1}{M^2} \cdot E\left\{ \left| \sum_{k=0}^{M-1} \left\{ \sum_{i=1}^{T} \left[\beta_i \cdot d(k-k_i) \otimes h_j\right] + w(k) \right\} \cdot x_j(\tau - \text{k}) \right|^2 \right\} \\ &= \frac{1}{M} \cdot E\left\{ \left| \sum_{i=1}^{T} \left[\beta_i \cdot d(k-k_i) \otimes h_j\right] \cdot x_j(\tau - \text{k}) \right|^2 \right. \\ &\qquad + \left| w(k) \cdot x_j(\tau - \text{k}) \right|^2 \\ &\qquad + \left(\sum_{i=1}^{T} \left[\beta_i \cdot d(k-k_i) \otimes h_j\right] \cdot x_j(\tau - \text{k}) \right) \\ &\qquad \times \left(w^*(k) \cdot x_j^*(\tau - \text{k}) \right) \\ &\qquad + \left(\sum_{i=1}^{T} \left[\beta_i^* \cdot d^*(k-k_i) \otimes h_j^*\right] \cdot x_j^*(\tau - \text{k}) \right) \\ &\qquad \left. \times \left(w(k) \cdot x_j(\tau - \text{k}) \right) \right\} \end{aligned}$$

Since $d(k)$ and $w(k)$ are mutually independent, the above equation can be simplified by using $E\{d(k)w^*(k)\} = E\{d^*(k)w(k)\} = 0$ such that

$$\begin{aligned} &\frac{1}{M} \cdot E\left\{ \left| \sum_{i=1}^{T} [\beta_i \cdot d(k-k_i)] \cdot x_j(\tau - \text{k}) \right|^2 + \left| w(k) \cdot x_j(\tau - \text{k}) \right|^2 \right\} \\ &= \frac{1}{M} \cdot E\left\{ \sum_{i=1}^{T} \left| \beta_i \cdot d(k-k_i) \cdot x_j(\tau - \text{k}) \right|^2 \right\} \\ &\quad + \frac{1}{M} \cdot E\left\{ \sum_{i\neq n}^{T} \beta_i \cdot \beta_n \cdot d(k-k_i) \cdot d^*(k-k_n) \right. \\ &\qquad \left. \times x_j(\tau - \text{k}) \cdot x_j^*(\tau - \text{k}) \right\} \\ &\quad + \frac{1}{M} \cdot E\left\{ \left(w(k) \cdot x_j(\tau - \text{k}) \right) \cdot \left(w^*(k) \cdot x_j^*(\tau - \text{k}) \right) \right\} \end{aligned} \tag{6}$$

Under assumption that $d(k)$ is i.i.d. random variables with zero-mean, then the second term of (6) goes to 0. In addition, since $w(k)$ and $x(k)$ are also mutually independent and by using properties such as $E\{|d(k)|^2\} = 1$, $E\{|x(k)|^2\} = 1$, and $E\{|w(k)|^2\} = \sigma^2$, (6) can be further simplified as follows;

$$\begin{aligned} &\frac{1}{M} \cdot E\left\{ \sum_{i=1}^{T} \left| \beta_i \cdot d(k-k_i) \cdot x_j(\tau - \text{k}) \right|^2 \right\} \\ &\quad + \frac{1}{M} \cdot E\left\{ \left(w(k) \cdot x_j(\tau - \text{k}) \right) \cdot \left(w^*(k) \cdot x_j^*(\tau - \text{k}) \right) \right\} \\ &\quad = \frac{1}{M} \cdot \left(\sum_{i=1}^{T} \left[{\beta_i}^2 \right] + \sigma^2 \right) \end{aligned} \tag{7}$$

Therefore, (5) can be represented as

$$E\left\{ \left| R_{r,x_j}(\tau) \right|^2 \right\} = \left(\alpha_j\beta_j \right)^2 \cdot E\left\{ \left| R_{x_j,x_j}(\tau) \right|^2 \right\} + \frac{1}{M} \cdot \left(\sum_{i=1}^{T} \left[{\beta_i}^2 \right] + \sigma^2 \right) \tag{8}$$

The auto-correlation properties of the Gold sequence are follows [15];

- Maximum auto-correlation value: $M = 2^n - 1$
- Correlation values excluding maximum correlation value $\in \{-1,\ -t(n),\ t(n)-2\}$ where $t(n) = 1 + 2^{\lfloor (n+2)/2 \rfloor}$
- $E\left\{ \left| R_{x_j,x_j}(\tau) \right| \right\} \approx \delta(\tau - c)$
- $E\left\{ \left| R_{x_j,x_j}(\tau) \right|^2 \right\} \approx \left(1 - \frac{1}{M} \right) \cdot \delta(\tau - c) + \frac{1}{M}$

By these properties of the Gold sequence, TINR for AWGN channel can be expressed by

$$\text{TINR} = 10\log_{10} \frac{M \cdot \left(\alpha_j \cdot \beta_j \right)^2 + \left(\sum_{i=1}^{T} \left[{\beta_i}^2 \right] + \sigma^2 \right)}{\left(\alpha_j \cdot \beta_j \right)^2 + \left(\sum_{i=1}^{T} \left[{\beta_i}^2 \right] + \sigma^2 \right)}$$

When the scaling factor corresponding to the injection level α_i goes to infinity ($\alpha_j \rightarrow \infty$), (9) approaches $10\log_{10}M$ that is the same as the processing gain described in Section III-A. On the other side, (9) approaches zero as the scaling factor corresponding to the injection level α_i goes to zero.

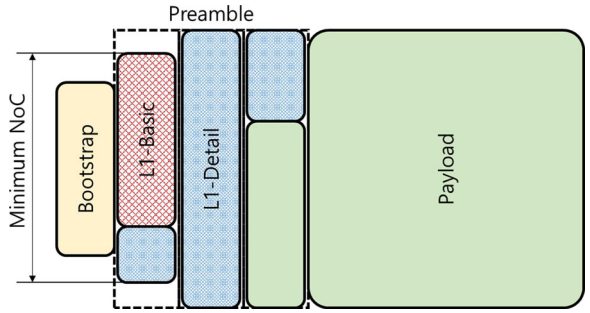

Fig. 3. ATSC 3.0 frame structure.

IV. ATSC 3.0 Frame Structure and Negative Impact on TxID Detection Performance

The practical implementation methods for detecting the ATSC 1.0 TxID signal were proposed in [17], [18]. In [17], 'ensemble average block' was used to aggregate and average multiple frames so that noise components can be dramatically reduced for the case of a sufficiently large number of averaging frames. It was shown that the ensemble average technique can provide 15 dB gain in terms of TINR through computer and laboratory test results. Although this ensemble average technique can be also applied to ATSC 3.0 TxID analyzer, its detection performance is seriously limited due to the frame structure of ATSC 3.0 described in Sections IV-A and B.

A. ATSC 3.0 Preamble Structure

As depicted in Figure 2, one or more TxID signals are injected into the first preamble symbol depending on FFT size. It implies that the OFDM waveform parameters of the preamble symbol such as FFT size, guard interval (GI) size, pilot boosting value, and pilot pattern, may affect the detection performance of TxID signal, and therefore it is necessary to investigate the structure of ATSC 3.0 frame in depth.

The ATSC 3.0 frame consists of the 3 types of symbols, as depicted in Figure 3. First, the bootstrap is located at the beginning of the frame, followed by preamble and payload. The bootstrap contains the essential information that enables the decoding of the first part of the preamble. The bootstrap symbols are designed to be independent of other ATSC 3.0 parts to facilitate future integration with other communication systems. In order to provide a robust performance and have a simple structure, auxiliary functions such as pilot insertion are excluded.

On the other hand, preamble and payload can have assorted combinations of OFDM parameters such as FFT size, GI, and scattered pilot (SP) pattern. ATSC 3.0 physical layer supports 12 selectable GI lengths and three FFT sizes of 8K, 16K, and 32K. For reliable channel estimation for various channel conditions, 16 SP patterns and 5 different pilot power boosting options are also provided. For each FFT size, the number of carriers (NoC) that can be determined by the number of carriers to be reduced (C_{red_coeff}) as shown in Table I. The value of NoC indicates the total number of carriers to be commonly used for pilot and payload. It is pre-determined that the first preamble symbol is set to have the smallest NoC value by default (i.e., $C_{red\_coeff} = 4$) since no specific signaling field for indicating NoC of the preamble is included in the bootstrap.

TABLE I
Number of Carriers

C_{red_coeff}	Number of Carriers (NoC)		
	8K FFT	16K FFT	32K FFT
0	6913	13825	27649
1	6817	13633	27265
2	6721	13441	26881
3	6625	13249	26497
4	6529	13057	26113

TABLE II
Preamble Pilot D_X for Each Combination of FFT Sizes and GI Values

GI Pattern	8K FFT	16K FFT	32K FFT
GI1_192	16	32	32
GI2_384	8	16	32
GI3_512	6	12	24
GI4_768	4	8	16
GI5_1024	3	6	12
GI6_1536	4	4	8
GI7_2048	3	3	6
GI8_2432	*N/A*	3	6
GI9_3072	*N/A*	4	8, 3
GI10_3648	*N/A*	4	8, 3
GI11_4096	*N/A*	3	3
GI12_4864	*N/A*	*N/A*	3

Pilot signals are inserted in the preamble and payload for frame synchronization, time synchronization, frequency synchronization, and channel estimation. ATSC 3.0 employs assorted kinds of preambles such as scattered, subframe boundary, common continual, additional continual, and edge pilots as shown in Figure 4. In the preamble part, only preamble pilot and common continual pilot (Common CP) are inserted. The value of separation of pilot carriers in the frequency direction, D_X, of the first preamble symbol is signaled by the 'preamble_structure' field in the last bootstrap symbol, as defined in Table II. The number of SPs is calculated as $\lceil \text{NoC}/D_X \rceil$ where $\lceil x \rceil$ is the least integer greater than or equal to x.

In addition, the number of Common CPs to be inserted into the preamble symbols is specified in Table III. In the case of the first preamble symbol, the number of Common CP is always selected as a value corresponding to $C_{red\_coeff} = 4$.

For example, if the OFDM parameters of the first preamble symbol are set to have 8K FFT size and 1024 GI interval, the number of active carrier (NoA) of the first preamble symbol can be calculated as follows;

$$\begin{aligned}\text{NoA} &= \text{NoC} - \text{No. of preamble pilots} - \text{No. of Common CPs} \\ &= 6529 - 2177 - 45 = 4307.\end{aligned}$$

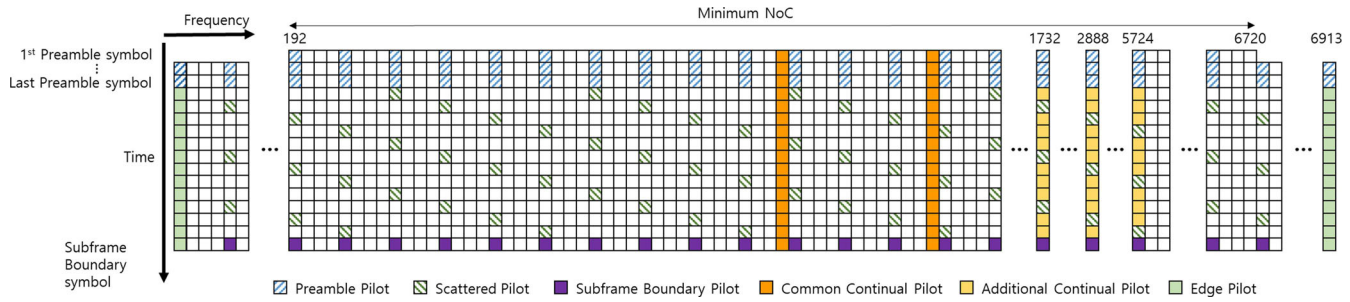

Fig. 4. Exemplary ATSC 3.0 frame structure for 8K FFT size and GI6_1536.

TABLE III
NUMBER OF COMMON CPS

C_{red_coeff}	8K	16K	32K
0	48	96	192
1	48	96	192
2	47	93	186
3	46	92	184
4	45	90	180

B. Limitation of Frame Averaging Technique

The detection performance of the TxID signal is greatly affected by the injection level, noise level, and reception channel environment. Hence, the injection level of the TxID signal should be carefully selected within a range that does not seriously impact the decoding performance of the host signal [19]. Since there is no normalization process after insertion of the TxID signal, an insertion of a high-level TxID signal can cause an increase in total transmission power. The transmit power of each transmitter is strictly regulated such that the actual transmit power should not generally exceed 1.05 times the granted transmit power. In order to meet this requirement, it is strongly recommended that the TxID injection level is selected from 15 dB to 45 dB. It should be also noted that, if a low TxID injection level is selected, the detection performance of the host preamble may be seriously degraded, and therefore it is desirable to insert a TxID signal whose injection level is as high as possible [19].

Due to such limited guideline for choosing TxID injection level, detection capability of TxID signal in a real field environment such as harsh channel condition may be insufficient. To overcome the limited reception power, ensemble average technique, that aggregates and averages a plurality of frames proposed in the ATSC 1.0 TxID analyzer [17], can be used to reduce noise level and increase TxID detection performance. It should be noted that the ensemble average technique is most effective when the host signal is completely random over frames. In ATSC 1.0 system, a significant performance gain from averaging technique can be achieved because only small portion of the host signal is repeatedly filled with the same signal over frame. However, the host signal of each frame in ATSC 3.0 system is not completely random and highly correlated each other due to preamble pilots and Common CPs as explained IV-A. In order to investigate the effect of the host signal's randomness on the TxID detection performance, let the randomness of the first preamble symbol be defined as follows;

$$\text{Randomness} = \text{NoA}/\text{FFT size}$$

The values of randomness of the first preamble symbol are calculated as shown in Table IV for various combination of FFT size and GI length. From the calculated randomness values, it can be seen that the randomness of the first preamble symbol varies from 52.58% to 76.65%.

As the insertion of TxID signal into the preamble is performed in the time domain after OFDM modulation, the conceptual block diagram considering the randomness of the host signal and insertion of the TxID signal can be depicted as Figure 5.

In order to investigate the relationship between the TxID detection performance and the randomness of the host signal,

TABLE IV
RANDOMNESS OF THE FIRST PREAMBLE SYMBOL FOR EACH COMBINATION OF FFT SIZE AND GI LENGTH

GI Pattern	8K FFT	16K FFT	32K FFT
GI1_192	74.16%	76.65%	76.65%
GI2_384	69.18%	74.16%	76.65%
GI3_512	65.86%	72.50%	75.82%
GI4_768	59.22%	69.18%	74.16%
GI5_1024	52.58%	65.86%	72.77%
GI6_1536	59.22%	59.22%	69.18%
GI7_2048	52.58%	52.58%	65.86%
GI8_2432	*N/A*	52.58%	65.86%
GI9_3072	*N/A*	59.22%	Dx=8; 69.45% Dx=3; 52.58%
GI10_3648	*N/A*	59.22%	Dx=8; 69.45% Dx=3; 52.58%
GI11_4096	*N/A*	52.58%	52.58%
GI12_4864	*N/A*	*N/A*	52.58%

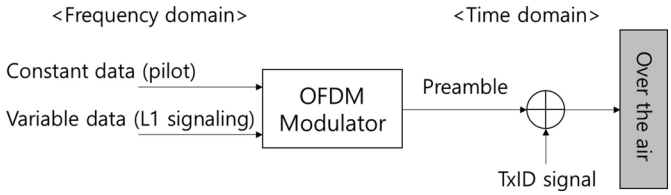

Fig. 5. Conceptual block diagram of TxID signal transmission.

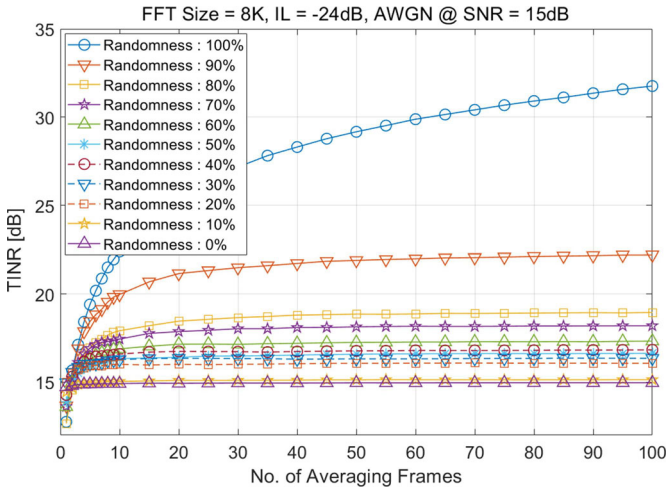

Fig. 6. Randomness vs. no. of averaging frames.

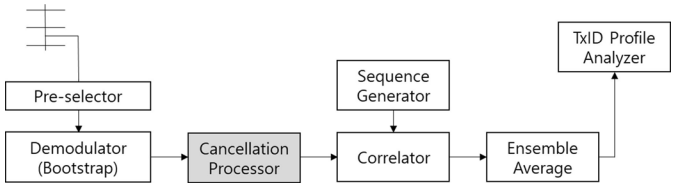

Fig. 7. Structure of advanced ATSC 3.0 TxID Analyzer.

computer simulation was conducted by assuming that the randomness of the host signal is defined as follows:

$$\text{Randomness} = \text{variable data}/(\text{variable data} + \text{constant data})$$

Computer simulations were performed when the amount of randomness was varied from 0% to 100% at 10% interval. As shown in Figure 6, for a single frame, the randomness of the host signal does not affect the TxID detection performance. As the number of averaging frames increases, however, it is observed that the randomness of the host signal has a significant impact on TINR performance. In particular, if the randomness is less than 80%, the TINR performance is saturated from 30 frames, so the gain obtained by frame averaging is up to 4 dB only, which is much worse than ATSC 1.0 case. This amount of gain may not be sufficient to ensure reliable detection of the TxID signal in the actual broadcasting environment. Therefore, a new approach is essential for the ATSC 3.0 TxID analyzer to overcome this limited detection performance.

V. Proposed Methods for Advanced TxID Analyzer

The structure of the proposed ATSC 3.0 TxID analyzer is depicted in Figure 7. The RF signals including TxID from multiple transmitters are received via the receiving antenna. The pre-selector rejects adjacent RF channels and remain the desired channel. The demodulator decodes the bootstrap signal and synchronizes with ATSC 3.0 frame by using the bootstrap signal. Once the bootstrap signal is successfully decoded, a value of 'preamble_structure' is obtained which indicates a basic structure of preamble such as FFT size, GI, pilot pattern, and L1-Basic protection mode. The detailed meaning of 'preamble_structure' is defined in Annex H of A/322 specification [1]. TxID sequence is generated and processed to be a TxID signal based on the acquired 'preamble_structure' information. The correlator correlates the received baseband signals with the generated TxID signal from the sequence generator. For aggregating and averaging the correlation values for multiple ATSC 3.0 frames, ensemble average technique can be additionally applied. Finally, the channel profiles for individual or multiple transmitters are displayed at the TxID profile analyzer.

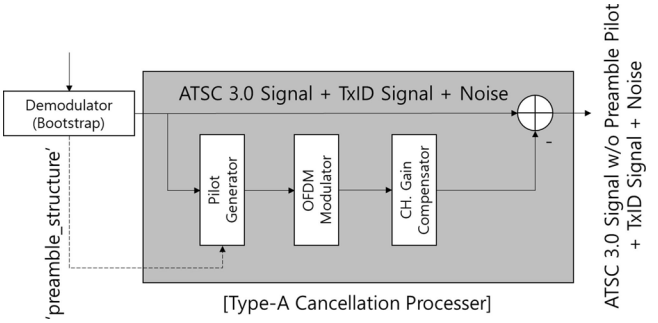

Fig. 8. Functional block diagram of Type-A cancellation processor.

In order to further improve the detection performance of ATSC 3.0 TxID signal, 'cancellation processor' is newly proposed between 'demodulator' and 'correlator' functional blocks. In this paper, three novel detection methods are proposed for the cancellation of ATSC 3.0 host preamble signal: Firstly, a pilot signal cancellation method, which is the simplest but can achieve a significant performance gain when the number of averaging frames is large enough. Secondly, a whole host preamble signal cancellation method provides the best performance, but it would induce much higher complexity than the first method due to LDPC decoding process of the preamble data part. Finally, the third method provides good performance with a reasonable complexity by using hard decision decoding for preamble data instead of full LDPC decoding.

A. Type A: Preamble Pilot Cancellation

As explained in Section IV-B, when the randomness of the host preamble signal is not sufficiently high, TxID detection performance is saturated even if a large number of frames is averaged. The key idea of this Type-A cancellation method is to remove constant components, i.e., pilot signals, in the first preamble symbol so that the frame averaging gain would be significantly increased compared to the conventional method. The detailed functional block diagram of this method is depicted in Figure 8. First of all, the pilot generator generates preamble pilot and common CP signals according to the value of 'preamble_structure'. The generated pilot signals are then modulated by the OFDM modulator which transforms frequency domain pilot signals into time domain signals. The channel gain compensator includes channel estimation and compensation of the received signal based on the estimated channel response. The channel response in frequency domain

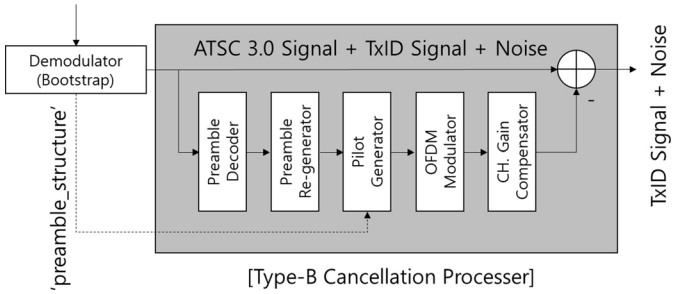

Fig. 9. Functional block diagram of Type-B cancellation processor.

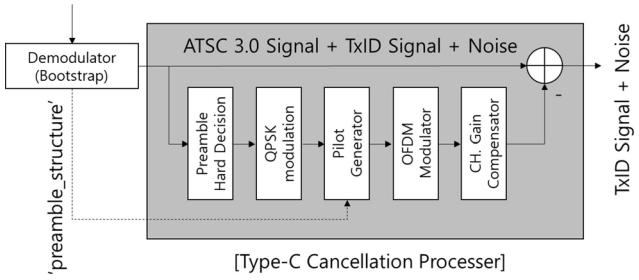

Fig. 10. Functional block diagram of Type-C cancellation processor.

is estimated by using the pilot signals of the first preamble symbol, and the compensated signal is generated by using the estimated channel response and the modulated pilot signals. The compensated signals are subtracted from the received baseband signals so that the components corresponding to pilot signals of the first preamble symbol are removed from the received signals. Therefore, the output of the cancellation processor consists of ATSC 3.0 signal without any pilot signals of the first preamble symbol, TxID signal, and noise.

B. Type B: Whole Preamble Cancellation With Full LDPC Decoding

The pilot signal cancellation method provides a significant performance gain in terms of TINR only if the number of averaging frames is large enough because the signal corresponding to the L1 signaling information is still present. In order to provide further improved performance even if frame averaging is not used, it is necessary to remove all the host preamble signals including the data and the pilot. To remove the data part of the preamble from the received signals, it needs to be decoded first by preamble decoding block which includes LDPC decoding. After the data in the preamble is decoded, signals corresponding to the decoded data are re-generated in accordance with the procedure of 'Protection for L1-signaling' in Section 6.5 of A/322 specification [1]. After preamble re-generator block, the same blocks in the Type-A cancellation processor are applied.

C. Type C: Hard Decision Base Whole Preamble Cancellation

Implementing the preamble decoding block in Type-B cancellation processor, especially LDPC decoder, results in high complexity at a TxID analyzer. To mitigate such high decoding complexity of LDPC decoding while maintaining good TINR performance, a hard decision decoding of the data in preamble is proposed. Constellations for the preamble signal are defined according to L1-Basic mode. For mode 1, 2, and 3, QPSK is used while high order constellations are used for higher modes of L1-Basic. Note that a lower mode of L1-Basic provides more robustness than higher modes. In the realistic broadcasting scenarios, L1-Basic mode 1 or 2 are highly demanded to provide enough robustness [20] in both fixed and mobile reception. Under this assumption, the Type-C cancellation method can provide comparable performance to the Type-B, but its complexity is much lower than the Type-B by omitting the LDPC decoding and preamble re-generation process. Therefore, considering both the implementation complexity and the TxID detection performance, the Type-C cancellation method is a good option for a low-cost TxID analyzer with having limited hardware computing power.

TABLE V
SYSTEM PARAMETERS

Parameter	Value
Baseband sample rate	6.912 MHz
Occupied BW	5.832 MHz
FFT size	[8K 16K 32K]
Guard interval	GI6_1536 (222.26 us)
No. of transmitters	[1 2 4]
Received signal separation	7 samples (1.0127 us)
Carrier-to-noise ratio	[15 18 21] dB
Channel	AWGN (Sim. and Lab.) AWGN-like (Field)

VI. TEST RESULTS

In this section, computer simulation results are provided in order to validate the equation derived in Section III-B. Computer simulation results for the conventional and three proposed schemes are also present to show that the proposed methods are superior to the conventional method. The laboratory test and field trial were performed to verify that the proposed method significantly improves the detection performance in real environment.

A. Comparison Between Calculation and Computer Simulation Results

Computer simulations were performed taking into account various injection levels, number of averaging frames, and number of transmitters constructing SFN. The system parameters for simulation are listed in Table V. The system bandwidth is set to 6 MHz so that the baseband sample rate and the occupied bandwidth are 6.912 and 5.832 MHz, respectively. GI is set to GI6_1536 being used for on-air UHDTV terrestrial broadcasting in the Republic of Korea. For multiple-transmitter case, the delay among signals received from each transmitter is assumed to be 7 samples (1.0127 us), respectively. Furthermore, the carrier-to-noise ratio (CNR) values are

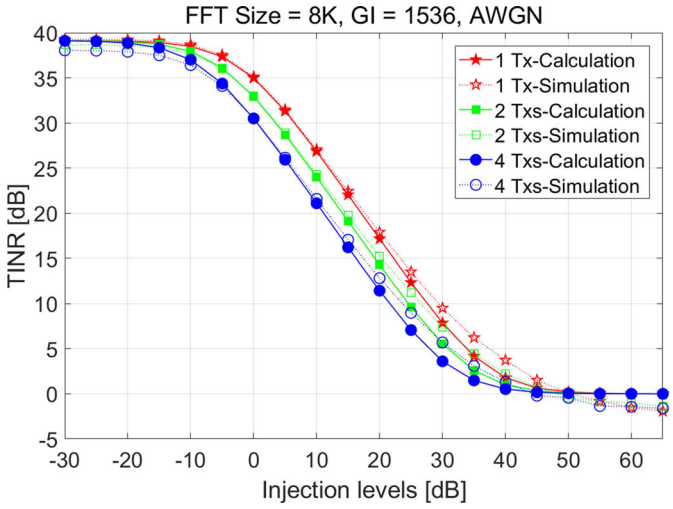

Fig. 11. Comparison of the calculated and the simulated TINR values for different number of transmitters under AWGN channel.

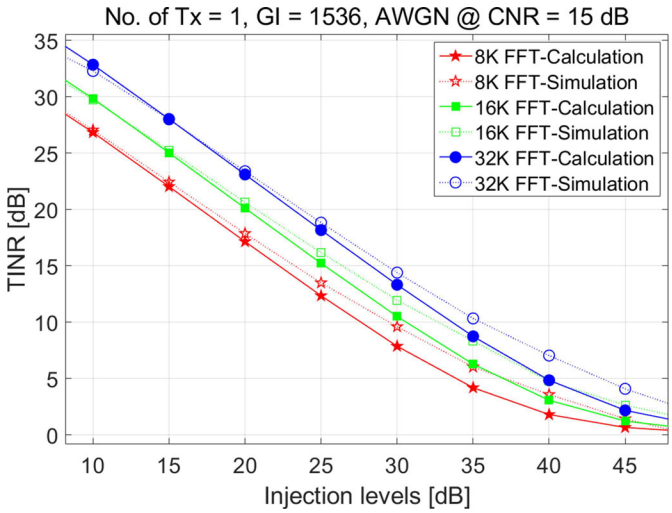

Fig. 12. Comparison of the calculated and the simulated TINR values for different FFT sizes under AWGN channel.

assumed to be 15, 18, and 21 dB for 1, 2, and 4 transmitters, respectively.

Figure 11 shows the performance comparison of the theoretical values calculated by (9) and computer simulated TINR values for a wide range of injection levels when 8K FFT size and no frame averaging technique are used. In the low injection level region, e.g., smaller than −20 dB, the TINR values are saturated with about 39 dB which is the processing gain inherently from the length of the Gold sequence, as explained in Section III-B. On the other hand, in the high injection level region, e.g., larger than 40 dB, the TINR values approach to 0 dB, as also explained in Section III-B. In the mid-range of the injection level, which is actually used in realistic broadcasting scenarios, the TxID detection performance is inversely proportional to the injection level and degraded by 3 dB when the number of transmitters is doubled. As shown in Figure 11, the calculated and simulated results are generally well-aligned in all range of injection levels.

Figure 12 shows the performance comparison of the theoretical values calculated by (9) and computer simulated TINR values for different FFT sizes of the preamble symbol when a single transmitter is present. As explained in Section II-B, the duplicated TxIDs are injected multiple times into the preamble symbol depending on the FFT sizes. It is shown that such repeated insertion of a TxID signal results in a roughly 3 dB performance gain when FFT size is doubled. However, for the high injection level region, all TINR values are converged to zero regardless of the FFT size. In the range from 10 dB to 30 dB, the TxID detection performance is inversely proportional to the injection level for all FFT sizes. As shown in Figure 12, the calculated results are generally well-aligned with the simulation results. It should be noted that 8K FFT size is generally selected for preamble in the realistic broadcasting scenarios, which implies that the repetition gain is predominantly not obtained in most cases.

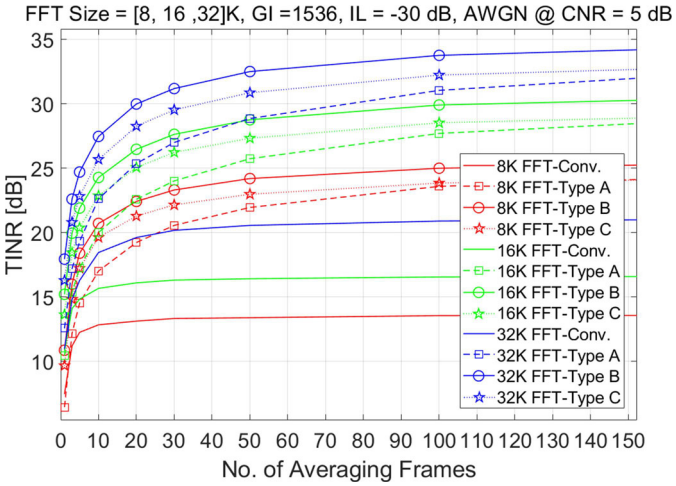

Fig. 13. Comparison of various detection method for different FFT sizes under AWGN channel.

B. Computer Simulation Results for Proposed Detection Methods

In order to compare the conventional and three proposed methods, computer simulation was performed, and results are shown in Figure 13 when different FFT sizes and various number of averaging frames are considered. To effectively show the gain from averaging frames, CNR is set to 5 dB which is not enough for TxID detection when no frame averaging is used. Due to constant components in the preamble symbol over consecutive frames, the conventional method provides only limited gain from frame averaging technique for all FFT sizes. The Type-A method, which is the pilot signal cancellation approach, provides significantly improved detection performances as the number of averaging frames is increased. For 100 averaging frames, this Type-A method offers 10 dB performance gain for all FFT sizes in terms of TINR compared to the conventional method. However, as shown in Figure 13, it provides no meaningful performance gain when no frame averaging is applied. On the other hand, the Type-B method,

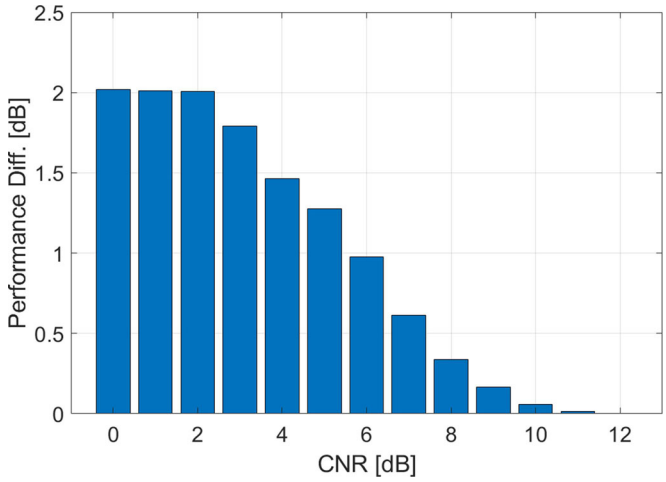

Fig. 14. Performance difference between Type-B and Type-C cancellation methods according to the reception SNR.

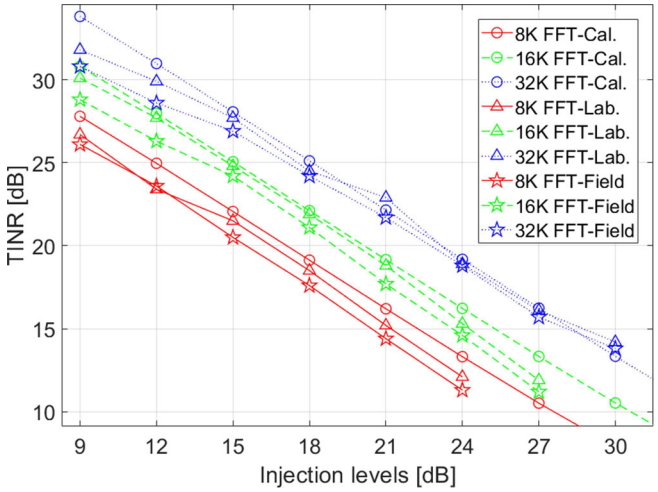

Fig. 15. Comparison of calculated, laboratory measured, and field measured TINR results for various FFT sizes.

which cancels out the whole host preamble signal based on full LDPC decoding, provides a steady performance improvement in all range of the number of averaging frames. Even if no frame averaging technique is used, the Type-B method offers 3.5, 4.5, and 7 dB performance gain over the conventional method for 8K, 16K, and 32K FFT sizes, respectively. The performance gain can be further improved when frame averaging is used. This Type-B method shows the best performance in all cases, but it has a high complexity mainly because of LDPC decoding.

The Type-C method, which is the hard decision decoding based whole host signal cancellation approach, shows good trade-off between TxID detection performance and complexity. The performance difference between Type-B and Type-C is approximately 1.5 dB for all range of the number of averaging frames. The amount of the performance degradation of Type-C method highly depends on the reception channel condition. It should be noted that the performance of the Type-C method is degraded mainly due to an incorrect cancellation of the host signal from errors occurred in QPSK demodulation. Figure 14 shows the simulated performance difference between the Type-B and Type-C methods according to CNR when the frame averaging technique is not used. As shown in Figure 14, the performance loss of the Type-C is negligible when the reception CNR is larger than 12 dB. As CNR is decreased, the performance difference is proportionally increased and saturated at approximately 2 dB. When the reception condition is fixed, these performance differences in the Type-B and Type-C methods are maintained for all ranges of the number of averaging frames as shown in Figure 13.

C. Laboratory and Field Test

In order to verify the performance of the proposed TxID detection methods, a hardware was implemented and tested in laboratory as well as realistic field environments. The implemented hardware includes the conventional and the proposed Type-B method. The system parameters for laboratory and field tests are the same as the computer simulations listed in Table V. ATSC 3.0 signal was generated at intermediate frequency (44 MHz) and up-converted to channel 50 (689 MHz). It is assumed that frame averaging technique is not used. For both laboratory and field tests, the average reception signal power and noise power were -79 and -97 dBm, respectively, in a single transmitter case.

For the field test, transmitter facilities including high power amplifier, channel filter, and directional transmitting antenna were installed at two different Jeju Techno Park buildings, Jeju island. The transmission power was 520 Watts effective isotropic radiated power and the height of the transmitting antenna was 21 meters above the ground level. In reception sites, the rooftop reception was conducted using test vehicle with 9 meters yagi (11 dB gain) antenna above the ground level.

Figure 15 shows the calculated, laboratory measured, and field measured results for various FFT sizes when a single transmitter is present. In laboratory and field tests, if the TINR value is less than 11 dB, it is considered as a detection failure because of insufficient discrimination capability of TxID peak. As shown in Figure 15, the results of calculation, laboratory test, and field test are generally well-aligned for all FFT sizes. In most cases, performance difference in calculated and field measured results is within 2 dB, whereas difference in laboratory and field measured results is around within 1 dB. The detection performance is proportionally reduced as the injection level of TxID signal is increased for all FFT sizes. The highest injection levels to ensure successful TxID detection in implemented hardware are measured at 24, 27, and 30 dB for 8K, 16K, and 32K FFT sizes, respectively.

Figure 16 shows the simulated and measured results for different number of transmitters in SFN when 8K FFT size is used for preamble. When two transmitters are present, the signal powers received from each transmitter are assumed to be equal to each other such that the combined signal power of the two transmitters is twice than the signal power of the single

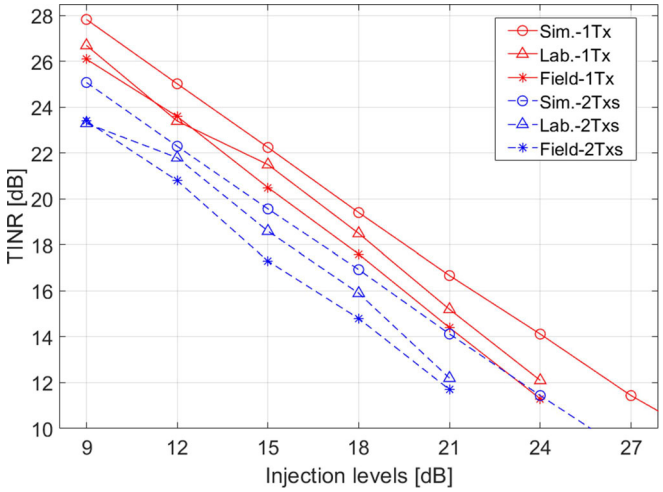

Fig. 16. Comparison of simulated, laboratory measured, and field measured TINR results for different number of transmitters.

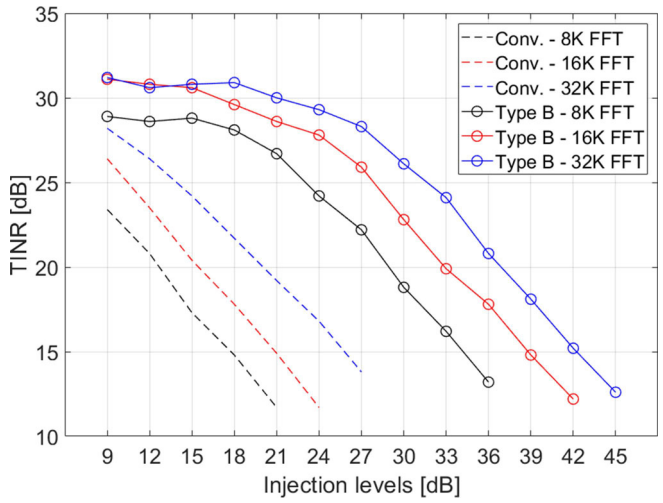

Fig. 17. Comparison of the conventional and proposed detection methods in SFN environment with 2 transmitters.

transmitter. For two-transmitter scenario, the TxID detection performance is 3 dB degraded compared to a single transmitter scenario for all injection level ranges. Therefore, the highest allowable injection level of two-transmitter scenario is reduced by 3 dB compared to the single transmitter scenario. The highest allowable injection level to ensure stable TxID detection is further reduced as the number of transmitters in SFN is increased.

Figure 17 shows the field measured performance difference in the conventional and the proposed Type-B methods. As shown in Figure 17, the proposed Type-B method outperforms the conventional method, and it enables to extend the maximum allowable TxID injection level for stable detection by approximately 15 dB for all FFT cases. On the other side, TINR performance gain at a given injection level is around within 10 to 15 dB. This enhanced detection capability enables to use higher TxID injection level or guarantees the stable TxID detection in multiple-transmitter scenarios.

VII. Conclusion

This paper presented the theoretical performance analysis of ATSC 3.0 TxID signal in comparison with the computer simulation results. In order to observe the limitation of the conventional TxID analyzer, the ATSC 3.0 frame structure was investigated in depth. The three TxID detection methods were newly proposed to overcome limitation of the conventional method, and each proposed method has pros and cons in terms of detection performance and complexity. Furthermore, one of the proposed methods was implemented in hardware and tested in laboratory and realistic field environment to verify that the proposed method is superior to the conventional one. According to the various test results, newly proposed methods can be used to efficiently design and manage SFN even when the interference from multiple transmitters is severe.

References

[1] *Advanced Television Systems Committee, Physical Layer*, ATSC Standard A/322, Sep. 2016.
[2] L. Fay, L. Michael, D. Gómez-Barquero, N. Ammar, and M. W. Caldwell, "ATSC 3.0 physical layer specification: An overview," *IEEE Trans. Broadcast.*, vol. 62, no. 1, pp. 159–171, Mar. 2016.
[3] L. Michael and D. Gómez-Barquero, "Bit interleaved coding and modulation for ATSC 3.0," *IEEE Trans. Broadcast.*, vol. 62, no. 1, pp. 181–188, Mar. 2016.
[4] M. Earnshaw, K. Shelby, H. Lee, Y. Oh, and M. Simon, "Physical layer framing for ATSC 3.0," *IEEE Trans. Broadcast.*, vol. 62, no. 1, pp. 263–270, Mar. 2016.
[5] *Advanced Television Systems Committee, System Discovery and Signaling*, ATSC Standard A/321, Mar. 2016.
[6] *Advanced Television Systems Committee*, ATSC Digit. Television Standard A/53, Sep. 1995.
[7] Digital Video Broadcasting, *Frame Structure Channel Coding and Modulation for a Second Generation Digital Terrestrial Television Broadcasting System (DVB-T2), V1.3.1*, ETSI Standard EN 302 755, Apr. 2012.
[8] L. Zhang *et al.*, "Layered division multiplexing: Theory and practice," *IEEE Trans. Broadcast.*, vol. 62, no. 1, pp. 216–232, Mar. 2016.
[9] S.-I. Park *et al.*, "Low complexity layered division multiplexing for ATSC 3.0," *IEEE Trans. Broadcast.*, vol. 62, no. 1, pp. 233–243, Mar. 2016.
[10] C. Regueiro *et al.*, "LDM core services performance in ATSC 3.0," *IEEE Trans. Broadcast.*, vol. 62, no. 1, pp. 244–252, Mar. 2016.
[11] S.-I. Park *et al.*, "Field comparison tests of LDM and TDM in ATSC 3.0," *IEEE Trans. Broadcast.*, vol. 64, no. 3, pp. 637–647, Sep. 2018.
[12] R. Scholtz, "The origins of spread-spectrum communications," *IEEE Trans. Commun.*, vol. COM-30, no. 5, pp. 822–854, May 1982.
[13] R. L. Pickholtz, D. Schilling, and L. B. Milstein, "Theory of spread-spectrum communications—A tutorial," *IEEE Trans. Commun.*, vol. COM-30, no. 5, pp. 855–884, May 1982.
[14] R. L. Peterson, R. E. Ziemer, and D. E. Borth, *Introduction to Spread-Spectrum Communications*. Upper Saddle River, NJ, USA: Prentice-Hall, 1995.
[15] D. V. Sarwate and M. B. Pursley, "Crosscorrelation properties of pseudo-random and related sequences," *Proc. IEEE*, vol. 68, no. 5, pp. 593–619, May 1980.
[16] D. Torrieri, *Principles of Spread-Spectrum Communication Systems*, Springer, 2005.
[17] S.-I. Park, J.-Y. Lee, H. M. Kim, and W. Oh, "Transmitter identification signal analyzer for single frequency network," *IEEE Trans. Broadcast.*, vol. 54, no. 3, pp. 383–393, Sep. 2008.
[18] S.-I. Park, H. M. Kim, and W. Oh, "Reception power estimation using transmitter identification signal for single frequency network," *IEEE Trans. Broadcast.*, vol. 55, no. 3, pp. 652–655, Sep. 2009.
[19] B.-M. Lim *et al.*, "Laboratory test analysis of TxID impact into ATSC 3.0 preamble," in *Proc. IEEE Int. Symp. Broadband Multimedia Syst. Broadcast. (BMSB)*, Jun. 2018, pp. 1–3.
[20] *Advanced Television Systems Committee, Guidelines for the Physical Layer*, ATSC Standard A/327, Oct. 2018.

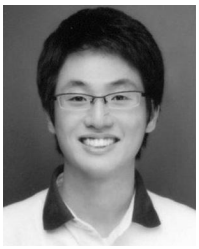

Sunhyoung Kwon (M'13) received the B.S. degree in electrical communications engineering from Information and Communications University, Daejeon, South Korea, in 2008, and the M.S. degree in electrical engineering from the Korea Advanced Institute of Science and Technology, Daejeon, in 2010. Since 2010, he has been with the Broadcasting System Research Group, Electronics and Telecommunication Research Institute, where he is currently a Senior Member of Research Staff. His research interests are in the area of digital broadcasting and communications.

Sung-Ik Park (A'07–M'08–SM'13) received the B.S.E.E. degree from Hanyang University, Seoul, South Korea, in 2000, the M.S.E.E. degree from POSTECH, Pohang, South Korea, in 2002, and the Ph.D. degree from Chungnam National University, Daejeon, South Korea, in 2011. Since 2002, he has been with the Broadcasting System Research Group, Electronics and Telecommunication Research Institute, where he is a Project Leader and a Principal Member of Research Staff. His research interests are in the area of error correction codes and digital communications, in particular, signal processing for digital television. He has over 200 peer-reviewed journal and conference publications, and multiple best paper and contribution awards for his work on broadcasting technologies. He currently serves as an Associate Editor for the IEEE TRANSACTIONS ON BROADCASTING and *ETRI Journal*, and a Distinguished Lecturer of IEEE Broadcasting Technology Society.

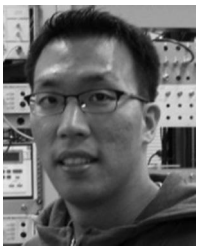

Jae-Young Lee (M'08–SM'17) received the B.S. degree (High Hons.) in electrical and computer engineering from Rutgers University in 2001, the M.S. degree in electrical and computer engineering from the University of Wisconsin at Madison, in 2003, and the Ph.D. degree in engineering science from Simon Fraser University in 2013. In 2003, he joined the Electronics and Telecommunications Research Institute, where he is currently a Principal Research Associate with the Broadcasting Systems Research Group. His research interests are in the areas of digital signal processing for various applications, including digital broadcasting, telecommunications, and human–computer interaction systems.

Bo-Mi Lim (M'15) received the B.S. degree from Ajou University, Suwon, South Korea, in 2008, and the M.S. degree from the Korea Advanced Institute of Science and Technology, Daejeon, South Korea, in 2010. Since 2010, she has been a Research Staff Member with the Broadcasting System Research Department, Electronics and Telecommunications Research Institute. Her research interests are in areas of wireless communication system design and digital broadcasting.

Sungjun Ahn (M'17) received the B.S. and M.S. degrees in electrical engineering from the Korea Advanced Institute of Science and Technology, Daejeon, South Korea, in 2015 and 2017, respectively. He has been with the Media Transmission Research Group, Electronics Research Institute, since 2017, where he is currently a Research Engineer. His research interests include stochastic geometry, signal processing, and optimization for wireless communication and digital broadcasting.

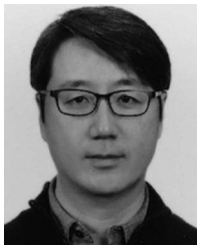

Joonhyuk Kang (S'00–M'03) received the B.S.E. and M.S.E. degrees from Seoul National University, Seoul, South Korea, in 1991 and 1993, respectively, and the Ph.D. degree in electrical and computer engineering from the University of Texas at Austin in 2002. He is currently a Faculty Member with the Department of Electrical Engineering, Korea Advanced Institute of Science and Technology, Daejeon, South Korea. From 1993 to 1998, he was a Research Staff Member with Samsung Electronics, Suwon, South Korea, where he was involved in the development of DSP-based real-time control systems. In 2000, he was with Cwill Telecommunications, Austin, TX, USA, where he participated in the project for multicarrier CDMA systems with antenna array. He was a Visiting Scholar with the School of Engineering and Applied Sciences, Harvard University, Cambridge, MA, USA, from 2008 to 2009. His research interest includes signal processing for cognitive radio, cooperative communication, physical-layer security, and wireless localization. He was a recipient of the Texas Telecommunication Consortium Graduate Fellowship from 2000 to 2002. He is a member of Korea Information and Communications Society and Tau Beta Pi (The Engineering Honor Society).